Journal of Fluorine Chemistry 132 (2011) 548–553

Contents lists available at ScienceDirect

Journal of Fluorine Chemistry

journal homepage: www.elsevier.com/locate/fluor

Effects of acid treatment on activated carbon used as a support for Rb and K catalyst for C_2F_5I synthesis and its mechanism

Aiqin Mao [a,b,c], Hua Wang [a], Linhua Tan [a], Xiangyang Nin [a], Renming Pan [a,*]

[a] School of Chemical Engineering, Nanjing University of Science and Technology, Nanjing 210094, China
[b] School of Materials Science and Engineering, Anhui University of Technology, Ma'anshan, Anhui 243002, China
[c] Anhui Key Laboratory of Metal Materials and Processing, Anhui University of Technology, Ma'anshan 243002, Anhui, China

ARTICLE INFO

Article history:
Received 28 March 2011
Received in revised form 22 April 2011
Accepted 30 May 2011
Available online 6 June 2011

Keywords:
Activated carbon
Acidic treatment
Surface oxygen group
C_2F_5I synthesis
Carbine

ABSTRACT

In the present work, the activated carbon (AC) support was treated with HCl, HNO_3 and HF solution. The order of catalyst dispersion was as follows: Rb–K/AC–HNO_3 > Rb–K/AC–HF > Rb–K/AC–HCl > Rb–K/AC. The same sequence was also observed for the amount of the acid surface oxygen groups on AC, but not for the basicity of the catalyst. The key role of acid treatment on AC surface chemistry and the basic sites, which are closely related to catalyst dispersion and basicity, is examined to rationalize these findings. On the other hand, a consideration of the reaction mechanism suggests that the reaction proceeds via CF_2 carbenes formed on the catalyst surface as intermediates, followed by carbine disproportionation to CF_3 radicals and CF_3CF_2 radicals, followed by reaction with I_2 to produce CF_3CF_2I, and it was also found that the Rb–K/AC–HCl catalyst with a high dispersion and moderate basicity was helpful for the enhancement of catalytic activity for C_2F_5I synthesis.

© 2011 Elsevier B.V. All rights reserved.

1. Introduction

Pentafluoroethyl iodide (C_2F_5I) is an important telogen for the telomerization of tetrafluoroethylene to long-chain perfluoroalkyl iodides, a raw material of resins, functional materials and an intermediate for medicines and agrochemicals [1,2]. A method for the preparation of C_2F_5I with low cost has attracted extensive attention recently. To date, C_2F_5I has been prepared by gap-type or continuous reaction of C_2F_4, iodine and iodine pentafluoride (IF_5) [3,4]. However, these methods have the potential hazard which originates in particular from the extremely reactive, toxic IF_5, and the increased rate of corrosion on the stainless steel apparatuses normally used. Recently, a continuous vapor phase process for the synthesis of C_2F_5I has been developed successfully by the reaction of C_2HF_5 and I_2 in the presence of an alkali or alkaline earth salt used as catalysts [5]. It makes the green production become possible. But to the best of our knowledge, in the open literature, little information about the catalyst technology was reported due to the complexities of its composition and structure.

Activated carbon (AC) has been widely used as a catalytic support, owing to its desirable properties, such as low cost, high surface area, abundant pore structure, stability in both acidic and basic media, possibility to modify the surface functionalities [6–8] and easily to recover the active component when supported on AC by burning off the support [9]. It has been well established in the literature that although the surface area and porous structure of AC may be very important for manufacturing carbon-supported catalysts with high performance, the surface oxygen groups, which form anchoring sites for metallic precursors as well as for metals, dominantly determine the properties of AC as a catalyst material [7,10,11]. What's more, the surface oxygen groups of AC, which are generally classified as acidic, neutral or basic groups, can be changed by the interaction between the carbon surface and the reactants adsorbed, such as the treatment with acids (HNO_3, HCl, HF, H_2SO_4, $HClO_4$ and so on) [8,12–15].

To reform the surface structure and suitability of AC as a support for Rb and K catalyst to synthesis C_2F_5I by the reaction of C_2HF_5, I_2 and O_2, we had modified the AC with HCl, HNO_3 or HF acid solutions to increase or to selectively remove some of the groups, and to obtain ACs with different surface properties. The pore structure and surface oxygen groups of the AC support before and after acid treatment were characterized by N_2 adsorption-desorption and Boehm titration. The dispersion and basicity of the catalysts were also investigated by X-ray diffraction (XRD), X-ray photoelectron spectroscopy (XPS), inductively coupled plasma atomic emission spectrometry (ICP-AES) and CO_2 temperature-programmed desorption (CO_2-TPD). On one hand, the effects of the different surface oxygen groups and textural properties of AC supports on the metal dispersion and then the basicity of the supported catalysts were analyzed and discussed. On the other

* Corresponding author. Tel.: +86 25 84315511; fax: +86 25 84315511.
E-mail address: panrenming@163.com (R. Pan).

0022-1139/$ – see front matter © 2011 Elsevier B.V. All rights reserved.
doi:10.1016/j.jfluchem.2011.05.032

Table 1
Effect of acid treatment on the ash content and support texture.

Sample	Ash (%)	S_{BET} (m^2/g)	V_{total} (cm^3/g)	V_{micro} (cm^3/g)	V_{meso} (cm^3/g)
AC	5.27	1008	0.539	0.458	0.081
AC–HCl	4.32	1010	0.540	0.481	0.059
AC–HNO_3	4.17	1046	0.575	0.535	0.040
AC–HF	1.28	1137	0.614	0.560	0.054

Table 2
pH_{slurry} and concentration of acidic and basic sites on AC.

Sample	Acidic sites (mmol/g)				Basic sites (mmol/g)	pH_{slurry}
	Carboxylic	Lactonic	Phenolic	Total		
AC	0.176	0.389	0.070	0.635	1.527	8.37
AC–HCl	0.092	0.248	0.411	0.751	0.507	6.87
AC–HNO_3	0.528	0.759	0.287	1.674	0.278	3.37
AC–HF	0.123	0.217	0.391	0.999	0.324	4.02

hand, the reaction mechanism of C_2F_5I and the activity of the catalysts has also been researched.

2. Results and discussion

2.1. Surface and pore structure of AC supports

Acid treatments of AC resulted in the removal of the inorganic constituents. The ash contents of the original and acid-treated AC supports are given in Table 1. As shown in Table 1, treatments of AC with HCl and HNO_3 nearly cause the same ash content reduction to about 4.2%, whereas HF treatment decreases the impurities greatly to about 1.28% ash content. The differences in the ash removal by the various acids can be explained as a result of the ability of the acids to remove different inorganic components. It has been reported that the content of the main impurities (Al, Si, Fe, Ti and K) in AC could be drastically diminished by HF. Other elements, such as Ca and S are mainly extracted by HCl. HNO_3 treatment could remove mineral matter such as S, Fe and Ca [18].

Table 1 also summarizes the S_{BET} and pore structure variations of the AC supports before and after acid treatment. The original AC has a high surface area and well-developed porosity, which is found to be mostly pronounced in the micropores. Interestingly, a slight increase in the micropore volume as well as surface area can be found both in the AC–HCl and AC–HNO_3, whereas HF treatment led to a significant increase in the micropore volume and surface area of the AC. From the weight losses of AC after acid treatment it is seen that HF eliminated most of the inorganic components in AC. Removal of these compounds resulted in the development of both micropore volume and surface area. Similar observations had also been reported by Wang and Zhu [18–20].

The pore size distributions of the all AC supports shown in Fig. 1 are complementary to the pore volume. It should be noted that the value of *y*-axis, being indicative of the pore volume, increases by acid treatment, especially in the case of HF, which is in good agreement with the ash analysis data (Table 1).

2.2. Surface oxygen groups on AC supports

The pH_{slurry} as an equivalent to the point of zero charge (PZC), gives an invaluable information about the surface oxygen groups and the electric surface charges [20]. It was well established that the surface oxygen groups of the AC support play a major role in determinating the extent and strength of interaction with the metal precursor during preparation of the catalyst. The surface oxygen groups on the AC surface are generally classified as acidic, basic, or neutral groups. Carboxylic, anhydride and lactone are acidic groups, while phenolic, carbonyl, quinine and ether groups are neutral or weakly acidic groups.

Table 2 shows the values of pH_{slurry}, concentration of the acidic and basic sites of various AC supports. As can be seen, the original AC exhibits a basic character, sample AC–HCl is neutral and the other two AC supports are both acidic. Sample AC–HNO_3 has the highest acidity, as expected. This is also consistent with the results reported by Gao and Wu [15], in which they found that HCl treatment can lead to the decomposition of carboxyl and lactone groups while increasing the relative amounts of the phenolic and carbonyl groups. In contrast, HNO_3 can increase the amounts of the acidic carboxyl and lactone surface groups. These results can also be identified by the results of Boehm titration.

Also can be shown that the amount of the lactonic groups is much higher than that of carboxylic groups and phenolic groups in all samples, and after being treated with the acids, the amount of surface acidic oxygen groups on AC increases according to the following sequence: AC–HNO_3 > AC–HF > AC–HCl > AC, which gives a good orientation about the pH_{slurry}. The increase in the surface acidic oxygen groups of the acid treatment AC supports may be contributed to getting rid of inorganic compounds which leaves defects or discontinuities for chemisorbing oxygen in air at room temperature [19,21] or decompose some groups to produce

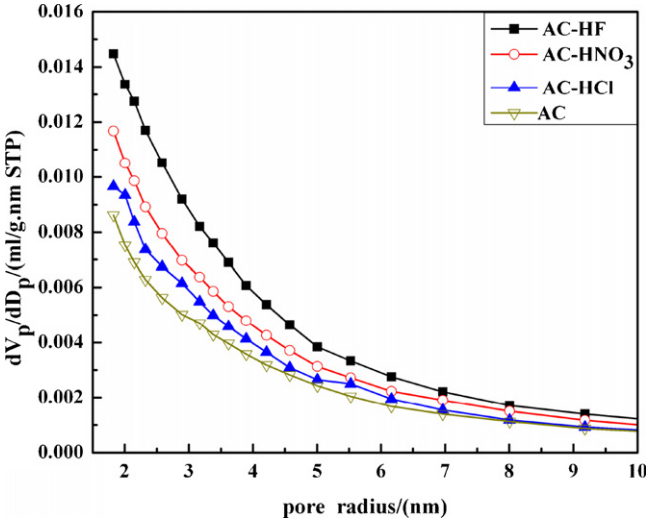

Fig. 1. Plots of the pore size distribution of AC samples.

Table 3
XPS results of the surface C and O concentrations of activated carbon.

Sample	C (%)	O (%)
AC	95.36	4.64
AC–HCl	95.23	4.87
AC–HNO_3	90.77	9.23
AC–HF	97.61	2.39

more acidic groups [15,16,20]. In addition, HNO_3 as an oxidant may also oxidize some complexes to produce acidic groups.

The concentration of oxygen and other elements on or near the AC surface can be measured directly by using the XPS technique. C and O surface concentrations on different AC supports given in Table 3 demonstrate that both HCl and HNO_3 treatments generally increase the surface oxygen content, while HF treatment has the opposite effect. It is important to keep in mind that surface oxygen in AC may be both inorganic and organic [20]. On one hand, acid treatment (especially HF) mainly gets rid of the inorganic oxides (see Table 1); on the other hand, acid treatment (especially HNO_3) adds the organic oxygen, which is reflected in the results of pH_{slurry} and Boehm titration.

2.3. Distribution of active catalyst species on AC supports

The XPS and ICP-AES techniques provide the invaluable information on the location and distribution of the active metal in the pore structure of the AC support [18]. Table 4 gives the XPS and ICP-AES analysis results of Rb/C and K/C quality ratios. It is found that the ratios of $(Rb/C)_{XPS}/(Rb/C)_{ICP}$ and $(K/C)_{XPS}/(K/C)_{ICP}$, indicative of the ratio of surface and bulk Rb and K concentration, are much lower than 1 for all catalysts except for the original AC-supported catalyst. This means that acid treatment improves the Rubidium and Potassium distribution in porous AC leading to more Rubidium and Potassium ions diffused into the inner pores, which can be confirmed by the XRD patterns of the catalysts (Fig. 2). The catalyst dispersion based on XPS and ICP-AES techniques follows the order: Rb–K/AC–HNO_3 > Rb–K/AC–HF > Rb–K/AC–HCl > Rb–K/AC, which corresponds to the sequence of the quantity of the surface acidic oxygen groups on the AC supports.

The XRD patterns of carbon-supported Rb–K catalysts are shown in Fig. 2. There are two broad diffraction peaks at $2\theta = 25.3^\circ$ and 43.1° of the turbostratic structure, which indicates that AC used is of a low graphitization degree [11]. The peaks at $2\theta = 21.7^\circ$ and 25.2° are the diffraction peaks of $RbNO_2$ and Rb_2O, the peaks at $2\theta = 35.2^\circ$ and 43.4° are $KF^\bullet 2H_2O$ and $KOH^\bullet H_2O$. Among the four samples, Rb–K/AC has the obvious diffraction peaks, while there is no any diffraction signal for the Rb–K/AC–HNO_3, Rb–K/AC–HCl and Rb–K/AC–HF samples. This suggests that Rubidium and Potassium located on AC–HNO_3, AC–HCl and AC–HF are highly dispersed, and the treatments of AC with the acids solution can improve the dispersion of Rubidium and Potassium on the AC. Xue and Zhu also reported that acidic treatment of carbons could improve the distribution of the metal, such as nickel and copper, on the carbon support because of more metal ions diffusing into the inner pores of carbons [11,18,20].

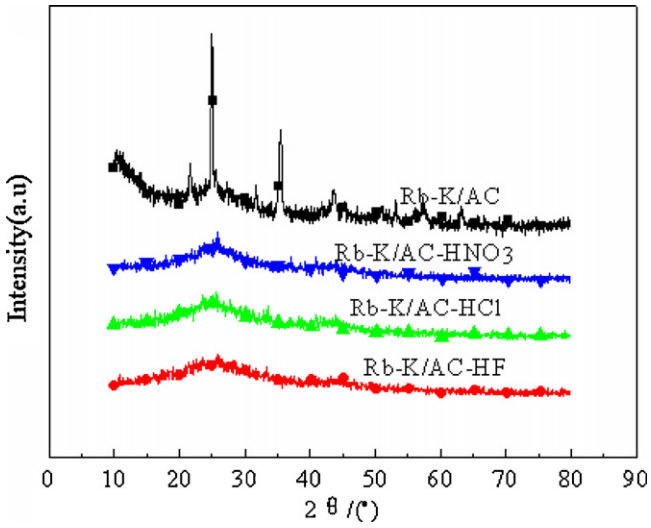

Fig. 2. XRD patterns of the carbon-supported Rb–K catalysts.

As seen above, the various AC supports may have different surface oxygen groups and consequently influence the diffusion of metal ions into the internal pore structure. Leon et al. [22,23] proposed that the interaction between metallic precursor and AC support depends on the amphoteric character of carbon material. At $pH > pH_{slurry}$ the carbon surface is covered by deprotonated carboxyl groups, the negatively charged surface then attracts and adsorbs cations from the solution; at $pH < pH_{slurry}$ it will attract anions. In other words, if the pH value of the impregnation solution is higher than the pH_{slurry}, then the adsorption of cations is favored. In this sense, these surface oxygen groups can be considered as the anchoring centers for the metallic precursor and its presence should favor higher dispersion. In this investigation, the access of the metallic precursor into the supports is carried out at the pH value of 7.65 of impregnation solution. Under these conditions, the pH value is higher than the pH_{slurry} of AC–HNO_3, AC–HCl and AC–HF, thus will dissociate the acidic groups on the AC surface, facing a negative charge to the solution, which favors for the adsorption of cationic species Rb^+ and K^+, and results in a high dispersion.

2.4. Surface basicity of the carbon-supported Rb–K catalysts

To investigate the base properties of the four catalysts, TPD profiles obtained after CO_2 adsorption are shown in Fig. 3. Two differentiated CO_2 desorption peaks can be observed, the low temperature peak with maximum at about 158 °C likely due to the bicarbonate species [24] resulting from the interaction of CO_2 with basic hydroxyl groups of AC or KF, the higher temperature peak with maximum at 412 °C, likely associated to decomposition of carbonate species [25] originating from the interaction of CO_2 with O^{2-}, which exhibits much higher thermal stability than the bicarbonate species.

Of note, acidic treatment of carbons decreases the area and the maximum temperature (T_{max}) of the low temperature peak of the Rb–K/AC catalyst. The area of the low temperature peak decreases

Table 4
Comparison between Rb/C and K/C quality radios from XPS and ICP analyses.

Catalyst	$(Rb/C)_{XPS}$	$(Rb/C)_{ICP}$	$(Rb/C)_{XPS}/(Rb/C)_{ICP}$	$(K/C)_{XPS}$	$(K/C)_{ICP}$	$(K/C)_{XPS}/(K/C)_{ICP}$
$RbNO_3$–KF/AC	0.324	0.1198	2.71	0.0487	0.0502	0.97
$RbNO_3$–KF/AC–HCl	0.0156	0.1186	0.13	0.0181	0.0521	0.35
$RbNO_3$–KF/AC–HNO_3	0.0108	0.1175	0.09	0.0165	0.0527	0.31
$RbNO_3$–KF/AC–HF	0.0147	0.1189	0.12	0.0176	0.0517	0.34

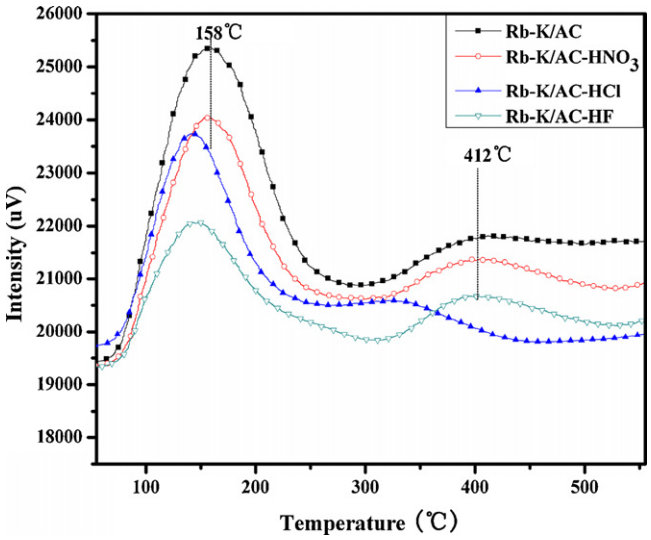

Fig. 3. CO_2-TPD curves of carbon-supported Rb–K catalysts.

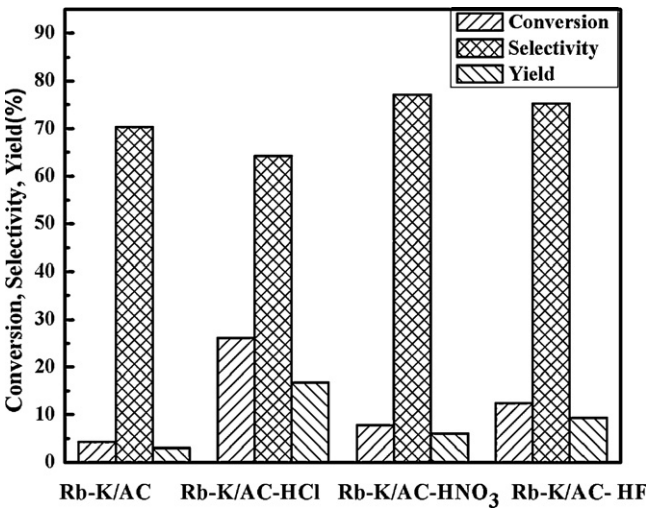

Fig. 4. Catalytic activity of the carbon-supported Rb–K catalysts.

obviously in the order: Rb–K/AC > Rb–K/AC–HNO_3 > Rb–KF/AC–HCl > Rb–KF/AC–HF, but no unambiguous correlation has been found between the dispersion and basicity of the catalysts. Keeping in mind the previous discussions of the basic sites of the AC supports and ratio $(K/C)_{XPS}/(K/C)_{ICP}$ of the catalysts, it seems reasonable that the basicity of all catalysts at low temperature is related to the dispersion of the active component K and the basic sites of AC. Although the dispersion of the active component K of untreated Rb–K/AC sample is the lowest, the basic sites of the untreated AC which can react with a strong acid and oxygen [26], are the highest. Compared to that in Rb–K/AC, the shift in T_{max} to lower temperature clearly indicates that the basic sites of the AC enhance the surface basicity. As seen in Fig. 3, the area of the high temperature peak increases with the dispersion of the active component Rb.

Therefore, it can be concluded that AC supports treated with HNO_3, HCl and HF increase the total amount of acidic sites, decrease the amount of the basic sites of AC, enlarge the dispersion degree of catalyst, and reduce the basicity of the catalyst at low temperature. These results show that K and Rb are preferable to exist in acid sites. Similar conclusion was also reported by Masai et al. [27]. They found that Lewis acid sites make the higher dispersion of Pd by the adsorption of the NH_3 and pyridine.

2.5. Catalytic reaction and the reaction mechanism

The conversion of C_2HF_5, selectivity and yield of C_2F_5I are shown in Fig. 4. It is seen that the Rb–K/AC catalyst demonstrates lowest conversion of C_2HF_5 and yield of C_2F_5I. For the catalysts treated by acids, the conversion of C_2HF_5 and yield of C_2F_5I enhance obviously, especially for the catalyst Rb–K/AC–HCl. Based on the catalytic conversion and yield, the order of the acid-treated catalysts are shown as follows: Rb–K/AC–HCl > Rb–K/AC–HF > Rb–K/AC–HNO_3, which is not related to the dispersion of catalysts (see Table 4) as well as the basicity of catalysts (see Fig. 3). These mean that in some cases, the activity does not improve in proportion to the dispersion, which suggests that other effects must be also considered. These effects could be the basicity of the catalysts.

Yang et al. [28,29] and Nagasaki et al. [30] have studied the mechanism for CF_3I synthesis by the reaction of CHF_3 and I_2, and suggested that the metal salts catalyzed the dehydrofluorination of CHF_3 to produce CF_2 carbene. The mechanism for C_2F_5I synthesis by the reaction of C_2HF_5 and I_2, and the mechanism for CF_3I synthesis have some similarities. The reaction proceeds of C_2F_5I by the following mechanism shown in Fig. 5. The first step causes HF to be eliminated from C_2HF_5 and CF_2 carbene is formed over the catalyst. Then CF_2 carbenes are disproportionation to CF_3 radicals. Next CF_2 carbenes are prior to reacting with CF_3 radicals for forming CF_3CF_2 radicals, and last the CF_3CF_2 radicals reacted with I_2 to produce CF_3CF_2I.

It has been reported [28] that CF_2 carbene combines with AC strongly. To examine the reaction mechanisms, the species of carbonaceous for the fresh and used Rb–K/AC–HCl catalysts are shown in Fig. 6. Karina et al. [31] has reported that the signal around 282.8 eV corresponds to carbon filaments produced from methane disproportion. The XPS studies reveal that the presence of carbon filaments peak of used catalyst around 282.1 eV are produced from the disproportion of CF_2 carbene ($3CF_2: \rightarrow 2CF_3^{\bullet} + C$). In addition, the C 1s XPS spectra of the used catalyst at binding energy of 290.9 eV and 292.5 eV can be assigned to CF_2 and CF_3, respectively which produced from the disproportion of C_2HF_5 ($C_2HF_5 \xrightarrow{cat.} 2CF_2 : + HF$) and CF_2 carbene. On the other hand, the surface area and pore volume especially micropores of the used catalyst decreases in comparison with the fresh catalyst due to the carbonaceous deposits on the used catalyst (see Table 5). Furthermore, in addition to the catalyst, a large quantity of carbonaceous powder was obtained when the used catalyst was

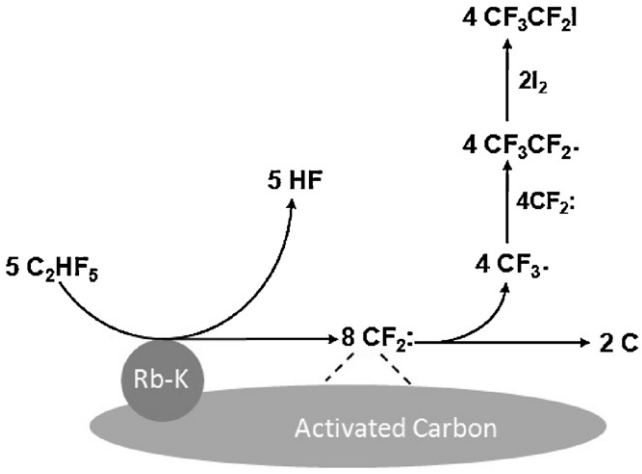

Fig. 5. Proposed reaction mechanism.

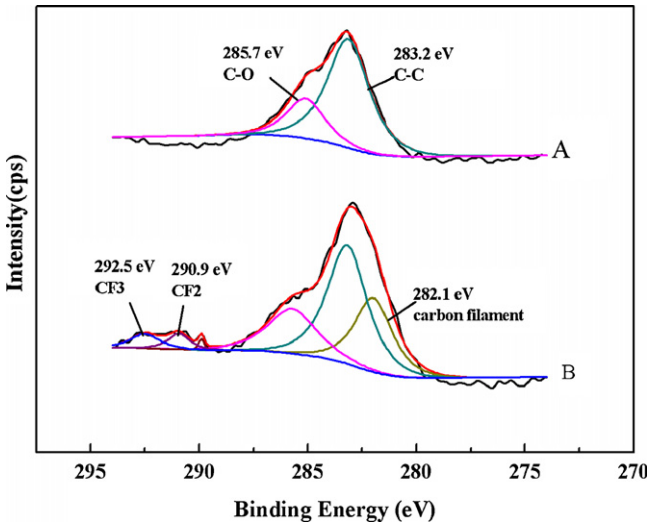

Fig. 6. XPS spectra of C 1s on Rb–K/AC catalysts. A: Fresh catalyst; B: used catalyst.

Table 5
Textual properties of Rb–K/AC catalyst.

Sample	S_{BET} (m^2/g)	V_{total} (cm^3/g)	V_{micro} (cm^3/g)	V_{meso} (cm^3/g)
Fresh catalyst	407	0.246	0.184	0.062
Used catalyst	138	0.124	0.064	0.061

recovered from the reactor. As a result, it is clear that the synthetic of C_2F_5I process is involved in this mechanism.

From the reaction mechanism, we can see that while the basicity of the catalysts is strong, it is difficult for the products HF and CF_3 radicals to be desorbed from the catalysts. So the Rb–K/AC–HCl catalyst which has a high dispersion and moderate basicity is beneficial to the synthesis of C_2F_5I.

3. Conclusions

Modification of activated carbon (AC) with different acid solution might result in various surface oxygen groups, which can enhance the anchoring interaction between AC supports and metal precursors and change the dispersion and basicity of the catalysts. The influence of HCl, HNO_3, and HF treatments on AC used as a support for Rb–K catalysts in the synthesis of C_2F_5I through the reacting of C_2HF_5, I_2 and O_2 was studied. The Rb and K dispersion follows a similar sequence of the total amount of the oxygen-containing surface groups on AC, and the basicity of the catalysts is related to the dispersion of the active component and the basic sites of AC. The different acid treatments produced various surface oxygen groups, which influenced the pore structures of the activated carbon, but to a lesser degree compared with their effects on catalyst dispersion and basicity.

Furthermore, a consideration of the reaction mechanisms suggests that the catalytic reaction proceeds via the disproportionation process of generated CF_2 carbene on the surface of the catalyst. The Rb–K/AC–HCl catalyst with a high dispersion and moderate basicity was beneficial to the preparation of C_2F_5I.

4. Experimental

4.1. Acid treatment of AC

A commercial granular coconut AC provided by Shanghai Activated Carbon Co., Ltd., China, was ground and sieved to the size of 0.85–1.00 mm prior to use. Then the AC was treated with different acidic solution, such as 2 M HCl, 2 M HNO_3 and 2 M HF for about 24 h at room temperature. After the treatment, samples were washed with distilled water and dried in air at 103–105 °C overnight. The ash content was determined by burning off the AC at 750 °C. The AC supports before and after acid treatment were then labeled as AC, AC–HCl, AC–HNO_3 and AC–HF, respectively.

4.2. Preparation of the catalyst

The catalysts were prepared by impregnating these supports with an aqueous solution of $RbNO_3$ and KF (Jiangxi Dongpeng New Materials Co., Ltd. and Sinopharm Chemical Reagent Co., Ltd., China, AR grade) at room temperature for about 6 h and dried by a rotary evaporator at about 80 °C for 4 h. Then the samples were dried in air at 110 °C overnight and finally calcined in N_2 flowing at 600 °C for 2 h. These samples were denoted as Rb–K/AC, Rb–K/AC–HCl, Rb–K/AC–HNO_3, Rb–K/AC–HF, respectively. The $RbNO_3$ and KF loading were 20 wt% and the mass ratio of $RbNO_3$ and KF is 2:1.

4.3. Characterization of AC and catalyst

The pH_{slurry} was measured as follows [16]: 1.0 g dry AC powder was added to 10 ml water and the suspension was stirred overnight. Then the sample was filtered and the pH_{slurry} was measured by a pH meter (Shang hai yueci, PHS-2C).

The content of surface oxygen groups on the AC was done following the Boehm titration [17]. 1 g sample was placed in 50 ml vial with 0.05 M aqueous solutions of NaOH, Na_2CO_3, $NaHCO_3$, respectively. After the vials were sealed and shaken for 24 h, the samples were filtered and 5 ml filtrate was pipetted. Excessive Na_2CO_3, $NaHCO_3$ and NaOH were titrated with 0.05 M HCl solution. The contents of acidic sites were calculated according to the assumption of the base solution, in which NaOH neutralized the carboxylic, phenolic and lactonic or lactol groups, Na_2CO_3 neutralizes the carboxylic and lactonic or lactol groups, and $NaHCO_3$ neutralized only carboxylic groups. The content of the surface basic sites was calculated by the amount of HCl reacted with the AC sample.

The textural structure was determined by N_2 adsorption–desorption at 77 K which was conducted using a gas sorption analyzer (Beckman Coulter SA 3100, USA). Samples were degassed for 2 h at 110 °C prior to the adsorption analysis. The specific surface area (S_{BET}) was calculated by the Brunauer–Emmett–Teller (BET) method. The total pore volume (V_{total}) was determined at a relative pressure $P/P_0 = 0.98$. The Barrett–Joyner–Halenda (BJH) method was used to calculate the mesopore volume (V_{meso}). The micropore volume (V_{micro}) was determined by subtracting V_{meso} from V_{total}.

The surface chemical composition was determined by XPS using a PHI-550 ESCA system. All spectra were acquired at a basic pressure of 2×10^{-7} Torr with Mg Kα excitation at 15 kV and recorder in the ΔE = constant mode with the pass energy of 50 and 100 eV. The total chemical composition was detected by ICP-AES. Three samples were measured in order to assure the accuracy.

The XRD measurements were conducted using a Bruker D8 Advance X-ray powder diffractometer, Cu Kα radiation was employed and the working voltage and current were 35 kV and 20 mA, respectively.

The basic properties of the catalysts were investigated by CO_2-TPD conducted on a BELSORP BEL-CAT-A instrument. In a typical experiment, certain catalysts placed in a U-shaped quartz tube were pretreated under He gas (50 cm^3/min) at 873 K for 30 min, then cooled down to 300 K. CO_2 instead of He at 10 mL/min was introduced for 1 h. The sample was flushed for 1 h to remove physical adsorbed CO_2. Then the desorbed CO_2 was measured by a

quadrupole mass spectrometer (Pfeiffer, OmniStar) from 300 K to 873 K at a heating rate of 10 K/min.

4.4. Activity testing

15 ml catalysts were packed into a fixed bed reactor (Inconel tubular, diameter 14 mm in and length 370 mm) and the reactor was heated to 600 °C under N_2 flow conditions, then the N_2 was changed to a mixture of gaseous raw materials (C_2HF_5 and O_2). Flow rate of the C_2HF_5 and O_2 were 18.6 ml/min and 2 ml/min, respectively, which was controlled by mass flow controller, and I_2 was provided by bubbling C_2HF_5 into molten I_2 which was placed in a stainless steel evaporator and heated up to 190 °C in an oil bath. After 4 h, the products passed through a $Ca(OH)_2$ solution and dried with $CaCl_2$. Then the products were analyzed by GC on line.

References

[1] V.A. Petrov, C.G. Krespan, US Patent 9 408072W (1994).
[2] D.J. Brauer, Y. Chebude, G. Pawelke, J. Fluorine Chem. 112 (2001) 265–270.
[3] K. Oharu, S. Kumai, JP Patent 9309847 (1997).
[4] H.B. Richter, P. Norbert, H. Rudolf, US Patent 6426439 (2002).
[5] J.M. Sage, FR Patent 2794456 (2000).
[6] S.X. Liu, X. Chen, X.Y. Chen, Z.F. Liu, H.L. Wang, J. Hazard. Mater. 141 (2007) 315–319.
[7] A.E. Aksoylu, M. Madalena, A. Freitas, M.F.R. Pereira, J.L. Figueiredo, Carbon 39 (2001) 175–185.
[8] G.G. Stavropoulos, P. Samaras, G.P. Sakellaropoulos, J. Hazard. Mater. 151 (2008) 414–421.
[9] J. Matos, J.L. Brito, L. Laine, Appl. Catal. A 152 (1997) 27–42.
[10] X.L. Zheng, Sh.J. Zhang, J.X. Xu, K.M. Wei, Carbon 40 (2002) 2597–2603.
[11] Y.Y. Xue, G.Z. Lu, Y. Guo, Y.L. Guo, Y.Q. Wang, Z.G. Zhang, Appl. Catal. B 79 (2008) 262–269.
[12] P. Chingombe, B. Saha, R.J. Wakeman, Carbon 43 (2005) 132–3143.
[13] H.S. Jazeyi, T. Kaghazchi, J. Ind. Eng. Chem. 16 (2010) 852–858.
[14] M. Gurrath, T. Kuretzky, H.P. Boehm, Carbon 38 (2000) 1241–1255.
[15] Z.M. Gao, Y. Wu, React. Kinet. Catal. Lett. 59 (1996) 359–366.
[16] H.H. Tseng, M.Y. Wey, Chemosphere 62 (2006) 756–766.
[17] H.P. Boehm, Carbon 40 (2002) 145–149.
[18] S.B. Wang, G.Q. Lu, Carbon 36 (1998) 283–292.
[19] S.B. Wang, Z.H. Zhu, Dyes Pigments 75 (2007) 306–314.
[20] Z.H. Zhu, L.R. Radovic, G.Q. Lu, Carbon 38 (2000) 451–464.
[21] R. Francisco, Carbon 36 (1998) 159–175.
[22] C.A. Leon y Leon, A.W. Scaroni, L.R. Radovic, J. Colloid Interface Sci. 148 (1992) 1–13.
[23] C.A. Leon y Leon, J.M. Solar, V. Calemma, L.R. Radovic, Carbon 30 (1992) 797–811.
[24] S. Scirè, C. Crisafulli, R. Maggiore, S. Minicò, S. Galvagno, Appl. Surf. Sci. 136 (1998) 311–320.
[25] C.L. Li, Y.L. Fu, G.Z. Bian, Acta Phys. Chim. Sin. 19 (2003) 902–906.
[26] H.L. Chiang, C.P. Huang, P.C. Chiang, J.H. You, Carbon 37 (1997) 1919–1928.
[27] M. Masai, H. Kado, A. Miyake, S. Nishiyama, S. Tsuruya, Stud. Surf. Sci. Catal. 36 (1988) 67–71.
[28] G.C. Yang, L. Shi, R.M. Pan, H.D. Quan, J. Fluorine Chem. 130 (2009) 231–235.
[29] G.C. Yang, X.Q. Jia, R.M. Pan, H.D. Quan, J. Fluorine Chem. 130 (2009) 985–988.
[30] N. Nagasaki, Y. Morikuni, K. Kawada, S. Arai, Catal. Today 88 (2004) 121–126.
[31] D. Karina, G. Víctor, M. Juan, Fuel 86 (2007) 1337–1344.